

Practical Realization of Optimal Auxiliary Frequency Control Strategy of Wind Turbine Generator

Ming Sun, *Student Member, IEEE*, Yong Min, Xuejun Xiong, Lei Chen, *Member, IEEE*, Le Zhao, Yuyao Feng, and Bingran Wang

Abstract—Adding the auxiliary frequency control function to the wind turbine generator (WTG) is a solution to the frequency security problem of the power system caused by the replacement of the synchronous generator (SG) by the WTG. The auxiliary frequency control using rotor kinetic energy is an economical scheme because the WTG still runs at the maximum power point during normal operation. In this paper, the functional optimization model of the auxiliary frequency control strategy of WTG is established. The optimal auxiliary frequency control strategy is obtained by solving the model numerically. As for the practical realization of the control strategy, the coordination of the auxiliary frequency control with the maximum power point tracking (MPPT) control is studied. The practical auxiliary frequency control strategy is modified to adapt to different power disturbances in the system, and the parameter setting method is also proposed. The sensitivity of system frequency to control parameters is studied. Finally, the simulation results verify the effectiveness and practicability of the proposed control strategy.

Index Terms—Power system frequency security, wind turbine generator, auxiliary frequency control, rotor kinetic energy, energy constraint.

I. INTRODUCTION

WITH the deterioration of the global environment, more attention is paid to new energy power generation including wind power, photovoltaic, and others. The new energy power generation is connected to the power system through power electronic devices, and under the conventional control strategy, it does not have the inertia and the

primary frequency control ability like the synchronous generator (SG). With the new energy generation constantly replacing the traditional SG, the inertia and frequency control ability of the power system decrease significantly, and the frequency security problem becomes critical [1]–[3], which seriously affects the power system security and the sustainable development of new energy generation.

To solve the problem, the auxiliary frequency control function is added to the wind turbine generator (WTG). Different modes to provide energy reserve for frequency control have been proposed, including the power reserve mode [4], [5] and rotor kinetic energy utilization mode [6]. The use of rotor kinetic energy can make the WTG operate in the maximum power point tracking (MPPT) mode and is more economical than the power reserve mode. Therefore, our research mainly focuses on the rotor kinetic energy utilization mode.

The power shortage and power surplus are two situations of frequency control in the system. For the auxiliary frequency control using rotor kinetic energy, when the system power is excessive, the WTG can reduce the electric power and achieve the effect of frequency regulation by adjusting the pitch angle or making the rotor accelerate away from the maximum power point, which is relatively easy to achieve. However, when the system power is insufficient, the WTG can only increase the electric power by reducing the rotor speed and releasing the kinetic energy stored in the rotor. Due to the limited kinetic energy of the WTG rotor, its electric power increase is temporary and more complex to realize. Therefore, this paper focuses on the auxiliary frequency control of the WTG using the rotor kinetic energy in the situation of power shortage in the system.

The auxiliary frequency control of WTG using rotor kinetic energy can be realized by supplementary power control, virtual SG control, or variable phase-locked loop (PLL) control. The supplementary power control is the easiest to realize and is studied in the paper. The widely studied control strategies are the frequency droop control (damping control) [7]–[11] and virtual inertia control [12]–[18]. The frequency droop control emulates the primary frequency control of the SG. The electric power increment of the WTG changes proportionally with the frequency deviation of the system. The virtual inertia control uses the frequency differential, i. e.,

Manuscript received: January 14, 2021; revised: March 11, 2021; accepted: June 15, 2021. Date of CrossCheck: June 15, 2021. Date of online publication: August 20, 2021.

This work was supported by State Grid Corporation of China (No. 52094020006V).

This article is distributed under the terms of the Creative Commons Attribution 4.0 International License (<http://creativecommons.org/licenses/by/4.0/>).

M. Sun, Y. Min, and L. Chen (corresponding author) are with State Key Laboratory of Power System and Generation Equipment, Department of Electrical Engineering, Tsinghua University, Beijing 100084, China (e-mail: sm16@mails.tsinghua.edu.cn; minyong@tsinghua.edu.cn; chenlei08@tsinghua.edu.cn).

X. Xiong, L. Zhao, and Y. Feng are with State Grid Shanghai Electric Power Research Institute, Shanghai 200437, China (e-mail: xiong_xj@sh.sgcc.com.cn; zhaole@sh.sgcc.com.cn; fengyuhao@sh.sgcc.com.cn).

B. Wang is with School of New Energy, Harbin Institute of Technology (Weihai), Weihai 264209, China (e-mail: 18911629163@189.cn).

DOI: 10.35833/MPCE.2021.000018



rate of change of frequency (ROCOF), as the input signal, and emulates the inertial response of the SG under power disturbance. In the initial stage of system frequency response (SFR), the frequency deviation is small, but the frequency differential is large. Therefore, the WTG with virtual inertia control can provide more power support in the initial stage. The combination of the frequency droop control and virtual inertia control is also called synthetic inertia control [19].

The WTG using rotor kinetic energy to participate in frequency regulation runs at the maximum power point during normal operation. When there is a power shortage in the system, the energy is released by rotor deceleration to participate in frequency regulation. However, the rotor speed has a lower limit. When the rotor speed is lower than the lower limit, the WTG will stop. Therefore, if the rotor speed drops to the lower limit, the WTG will terminate the auxiliary frequency control function and the electric power of WTG decreases instantaneously, which is a negative power impact on the power system and results in a secondary drop in the system frequency. Therefore, this issue must be considered when designing the auxiliary frequency control of the WTG [20]. In [21] and [22], the rotor speed recovery is considered in the design of the control strategy. In [23], the synthetic inertia control is believed to be approximately the optimal frequency control strategy of power electronic equipment under energy constraints.

In the existing research, the common idea of designing the auxiliary frequency control strategy of WTG is to make the WTG emulate the response of SG, including inertial response and primary frequency control response. However, whether this kind of emulation is necessary or optimal is rarely studied. The inertial response of SG is its inherent physical characteristic, and the primary frequency control of SG has the disadvantage of slow response. The controllability of the electric power of SG in the electromechanical time scale is relatively poor. On the contrary, the control of the electric power of the WTG with a power electronic interface is much faster and more flexible than that of SG. However, WTG has the defect of limited energy for frequency support. Therefore, the research of the auxiliary frequency control strategy of WTG should not be limited to the framework of virtual inertia control or frequency droop control. It should make full use of the advantages of rapidity and flexibility of WTG electric power while considering the energy constraint to obtain better SFR.

In our previous research [24], the optimal auxiliary frequency control strategy of WTG is obtained by electric power curve optimization and curve fitting. In this paper, the functional optimization model of WTG auxiliary frequency control is established. The form of the optimal auxiliary frequency control strategy of WTG is obtained by numerically solving the model and then transfer function fitting. Furthermore, the practical realization of the auxiliary frequency control strategy is studied. The simulation results verify the effectiveness and practicability of the proposed practical auxiliary frequency control strategy. The main contributions are as follows.

1) The functional optimization model of the auxiliary fre-

quency control strategy of WTG is established and numerically solved. The control strategy is obtained by transfer function fitting.

2) The practical design of the optimal auxiliary frequency control strategy of WTG is proposed. The coordination of the optimal auxiliary frequency control with the MPPT control is studied. The auxiliary frequency control strategy of WTG for the situation of power surplus and frequency rising is studied. The parameter setting method in practical power systems is proposed and discussed in detail.

3) The influence and sensitivity of control parameters of the practical optimal auxiliary frequency control strategy of WTG on the system frequency are studied to provide guidance for parameter setting.

4) The feasibility and robustness of the proposed control strategy of WTG are studied.

The remainder of the paper is organized as follows. Section II presents the theoretical basis of the optimal auxiliary frequency control strategy of WTG. Section III designs the practical optimal auxiliary frequency control strategy of WTG. Section IV studies the influence on system frequency of control parameters and their sensitivity to system frequency. Section V presents the simulations that verify the effectiveness of the proposed control strategy. Section VI presents the conclusions.

II. THEORETICAL BASIS OF OPTIMAL AUXILIARY FREQUENCY CONTROL STRATEGY OF WTG

In this section, the theoretical basis of the optimal auxiliary frequency control strategy of WTG is introduced.

As shown in Fig. 1, the system model for theoretical analysis of auxiliary frequency control of WTG consists of one SG, one WTG, and one load.

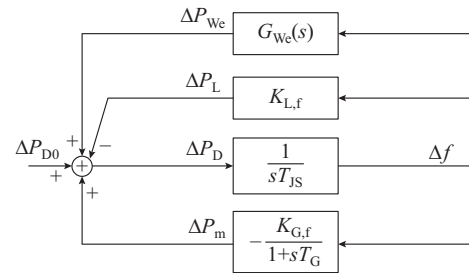


Fig. 1. Diagram of system model for theoretical analysis of auxiliary frequency control of WTG.

Our goal is to find an optimal control strategy for WTG. This is actually a functional optimization problem. The optimization goal is to maximize the frequency nadir Δf_{\min} , which is a functional (a mapping from a set of functions, i.e., control strategy $G_{Wc}(s)$, to a numerical value), as shown in (1). $G_{Wc}(s)$ is the function that needs to be optimized. The constraints are presented in (2)-(10).

$$\max_{G_{Wc}(s)} (\Delta f_{\min}) \quad (1)$$

$$\frac{d\Delta f}{dt} = \frac{1}{T_{JS}} (\Delta P_{D0} + \Delta P_m - \Delta P_L + \Delta P_{Wc}) \quad (2)$$

$$\frac{d\Delta P_m}{dt} = -\frac{1}{T_G} (\Delta P_m + K_{G,f}\Delta f) \quad (3)$$

$$\Delta P_L = K_{L,f}\Delta f \quad (4)$$

$$T_{JW}\omega_w \frac{d\omega_w}{dt} = P_{Wm} - P_{We} \quad (5)$$

$$P_{Wm} = f(\omega_w) = K \left(\frac{A}{\omega_w} + B \right) e^{\frac{C}{\omega_w}} \quad (6)$$

$$\omega_w \geq \omega_{wmin} \quad (7)$$

$$\omega_w(t_{end}) = \omega_{w0} \quad (8)$$

$$P_{We}(t_{end}) = P_{We0} \quad (9)$$

$$P_{We}(t_0) \geq 0 \quad (10)$$

where Δf is the system frequency deviation from the nominal value; ΔP_{D0} is the power disturbance in the system; ΔP_m is the frequency regulation power of SG; ΔP_L is the frequency regulation effect power of the load; ΔP_{We} is the frequency regulation power of WTG; ω_w is the rotor speed of WTG; P_{Wm} is the mechanical power of WTG; P_{We} is the electric power of WTG; T_{JS} is the inertia time constant of SG; $K_{G,f}$ is the power-frequency coefficient of SG prime mover; T_G is the time constant of SG prime mover and governor; $K_{L,f}$ is the power-frequency coefficient of the load; T_{JW} is the inertia time constant of WTG; K , A , B , and C are the coefficients of wind power captured by WTG; ω_{wmin} is the lower limit of WTG rotor speed; ω_{w0} is the WTG rotor speed before frequency regulation; P_{We0} is the WTG electric power before frequency regulation; t_0 is the start time of primary frequency regulation; and t_{end} is the end time of primary frequency regulation.

Constraints (2), (3), (4), (5), (6), and (7) represent the system frequency characteristic, the frequency regulation of SG, the frequency regulation effect of the load, the rotor motion equation of WTG, the mechanical power of WTG, and the minimum speed limit of WTG, respectively. WTG has to return to the original operating point before frequency regulation so that (8) and (9) are obtained. The maximum ROCOF is not worse than that of the situation when WTG does not participate in frequency regulation, so that (10) is obtained. A detailed explanation of the constraints can be found in [24].

It is difficult to obtain an analytical solution of the above functional optimization model. Therefore, a numerical method is required to solve the functional optimization problem.

In [24], the WTG electric power ΔP_{We} is set as optimizing decision variables, and then the functional optimization problem is transformed to the problem of finding the optimal electric power curve, which is further discretized to a series of points. The optimal electric power curve and optimal SFR are obtained. The optimal control strategy is obtained by curve fitting. However, this curve fitting method is not rigorous enough. In this paper, a numerical solution to the functional optimization model is proposed.

According to [24], the optimal SFR is shown in Fig. 2, which can be divided into two stages (stage 1 and stage 2). In stage 1, the system frequency decreases and remains unchanged. In stage 2, the system frequency recovers to steady-state frequency.

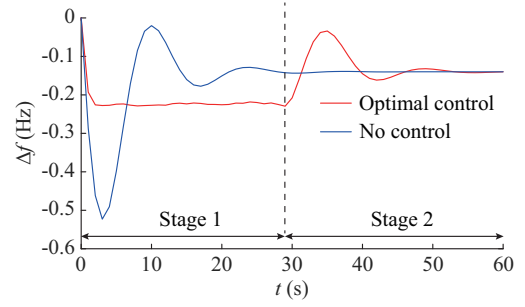


Fig. 2. Optimal SFR.

The SFR in stage 1 is almost a first-order response. The initial ROCOF is almost the same as that of the situation when WTG does not participate in frequency regulation. Therefore, the transfer function from ΔP_{D0} to Δf can be obtained as:

$$G_{sys}(s) = \frac{1}{K_{sys} + sT_{JS}} \quad (11)$$

where K_{sys} is an undetermined parameter. We only need to determine the form of control strategy. Therefore, the system model can be simplified as shown in Fig. 3.

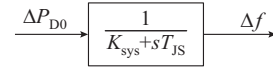


Fig. 3. Diagram of simplified system model.

Comparing Fig. 1 with Fig. 3, we can obtain:

$$-K_{L,f} - \frac{K_{G,f}}{1 + sT_G} + G_{We}(s) = -K_{sys} \quad (12)$$

Thus,

$$G_{We}(s) = -K_{sys} + K_{L,f} + \frac{K_{G,f}}{1 + sT_G} = -\left(K_{WD1} - \frac{K_{WD2}}{1 + sT_{WD}} \right) \quad (13)$$

where $K_{WD1} = K_{sys} - K_{L,f}$; $K_{WD2} = K_{G,f}$; and $T_{WD} = T_G$.

Accordingly, we can obtain the optimal auxiliary frequency control strategy as shown in (14), which needs further practical design before application.

$$\Delta P_{We}(s) = -\left(K_{WD1} - \frac{K_{WD2}}{1 + sT_{WD}} \right) \Delta f(s) \quad (14)$$

III. DESIGN OF PRACTICAL OPTIMAL AUXILIARY FREQUENCY CONTROL STRATEGY OF WTG

In Section II, an optimal auxiliary frequency control strategy is obtained by numerically solving the functional optimization problem. However, the coordination with MPPT control is also very important for the practical realization of the optimal auxiliary frequency control strategy. The method for switching between the MPPT mode and the optimal auxiliary frequency control mode needs further investigation.

In this section, the practical optimal auxiliary frequency control strategy of WTG is designed. The detailed flow chart of the control strategy and the methods to determine control parameters are presented. The advantages of the proposed control strategy are also discussed.

A. Flow Chart of Practical Optimal Auxiliary Frequency Control Strategy

In the beginning, the WTG operates in the MPPT mode. To obtain the time for WTG to switch from MPPT mode to frequency regulation mode, a dead zone is set for the frequency. When the system frequency is inside the dead zone, WTG does not participate in the frequency regulation, and its electric power is determined by the MPPT power order, i.e., $P_{We} = K\omega_W^3$, where K is the parameter of the MPPT control of WTG. Once the frequency is out of the dead zone, the WTG electric power at this time is taken as the reference value, denoted as P_{We0} . After checking that the rotor speed is within the proper range, which means there is rotor kinetic energy for frequency regulation, the WTG electric power is changed to (15), or the control mode will be switched to MPPT mode immediately.

$$P_{We} = P_{We0} + \Delta P_{We} \quad (15)$$

Notice that with the decrease of rotor speed, the MPPT power order will decline. Therefore, when WTG switches to the frequency regulation mode, P_{We0} has to remain unchanged until WTG switches back to the MPPT mode.

The scenarios of frequency disturbance include the frequency drop and frequency rise. It is necessary for the auxiliary frequency control strategy to consider both scenarios. Therefore, the control strategies in stage 2 are different. When the system frequency decreases and the frequency regulation signal is smaller than the MPPT signal, or the system frequency increases and the frequency regulation signal is bigger than the MPPT signal, WTG switches back to the MPPT mode. The flow chart of the practical optimal auxiliary frequency control strategy of WTG is shown in Fig. 4.

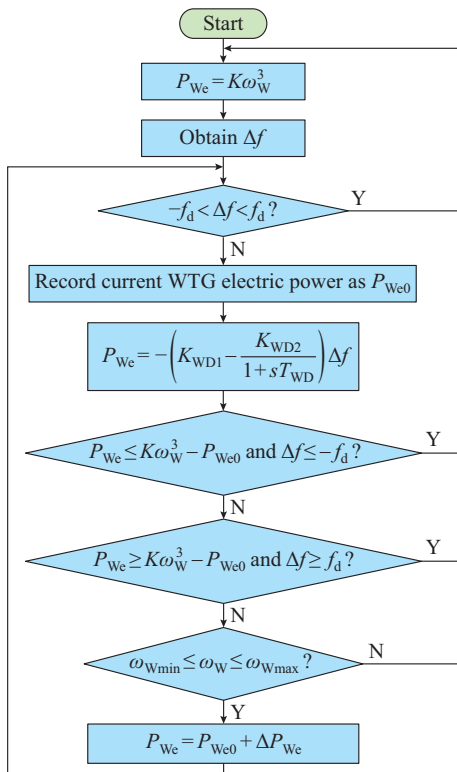


Fig. 4. Flow chart of practical optimal auxiliary frequency control strategy of WTG.

B. Parameter Setting of Judgement Conditions

Since the installed capacity of thermal power is higher than that of hydro power in most power systems in China, the frequency dead zone value of WTG f_d can be set to be the frequency dead zone value of the thermal generator, which is ± 0.033 Hz for better coordination between the WTG and the thermal generator. If f_d is too small, the WTG will start the frequency regulation earlier than the SG. As a result, the frequency regulation capacity of the WTG is exhausted too quickly and the WTG will terminate the frequency regulation too early. Such a situation is not good for SFR. If f_d is too big, WTG will start the frequency regulation too late and its advantages of power control rapidity cannot be fully utilized. Therefore, f_d is set to be the same as the frequency dead zone value of the thermal generator. During normal operation, the rotor speed of WTG also changes according to the wind speed, so it is not a problem for WTG to change its rotor speed frequently for frequency regulation.

C. Parameter Setting of K_{WD2} and T_{WD}

According to [24], K_{WD2} should be equal to $K_{G,f}$ and T_{WD} should be equal to T_G to achieve better coordination between the frequency regulation of WTG and SG. This means K_{WD2} and T_{WD} are decided by SG parameters. However, in real power systems, the frequency regulation characteristic of SGs is very complex. Different SGs have different parameters. It is difficult to obtain the equivalent $K_{G,f}$ and T_{WD} from SG parameters directly. Therefore, for practical use, the following procedure can be adopted.

- 1) Establish the governor and prime mover models of SGs.
- 2) Input the step signal of frequency $\Delta f(t) = cu(t)$ to the model, where $u(t)$ is the unit step signal and c is the preset magnitude.
- 3) Add the power increment signals of each governor and prime mover to obtain the total power increment signal $\Delta P_{m\Sigma}$.
- 4) Fit $\Delta P_{m\Sigma}$ with an exponential function, and obtain $\Delta P_{m\Sigma} = c\hat{K}_{G,f}(1 - e^{-t/\hat{T}_G})u(t)$, where $\hat{K}_{G,f}$ and \hat{T}_G are the fitting parameters.
- 5) Obtain $K_{WD2} = \hat{K}_{G,f}$ and $T_{WD} = \hat{T}_G$.

D. Parameter Setting of K_{WD1}

The optimal K_{WD1} is decided by K_{WD2} and T_{WD} . If K_{WD1} is larger, the frequency support effect will be better (the frequency nadir will be higher), but the rotor speed of WTG will drop faster. The rotor speed will stop dropping when the electric power is equal to the mechanical power. Therefore, if the rotor speed is higher than the lower limit at the moment when the electric power is equal to the mechanical power, the rotor speed will not reach the lower limit. K_{WD1} should be as big as possible in the feasible region. K_{WD1} can be decided by trail in the system.

Apply a power shortage disturbance ΔP_{D0} on the system, and find the biggest K_{WD1} that can guarantee the rotor speed higher than the lower limit. The ΔP_{D0} used to determine K_{WD1} should consider the most severe power shortage that may occur. The K_{WD1} obtained from more severe power shortage can be adapted to the situation with a less severe power shortage.

To avoid the rotor speed of WTG in the proposed control strategy decreasing below the lower limit, K_{WD1} should be adjusted according to the rotor speed of WTG, while K_{WD2} and T_{WD} should remain the same. When the wind speed decreases during operation, K_{WD1} should decrease as well. Furthermore, K_{WD1} should be conservative to deal with the situation that the wind speed decreases during the frequency regulation process of WTG. The degree of conservatism depends on the possible fluctuation range of wind speed in the time scale of primary frequency regulation.

E. Advantages of Proposed Control Strategy

The proposed control strategy not only realizes the coordination between WTGs and SGs in the frequency regulation [24], but also has the following advantages.

- 1) The WTG switches smoothly between the MPPT mode and frequency regulation mode, especially from the frequency regulation mode to the MPPT mode, to avoid secondary frequency drop.
- 2) The control strategy can be applied to both scenarios of frequency drop and frequency rise.
- 3) The control strategy is concise and easy to implement.
- 4) The WTG will return to the original operating point after the frequency regulation.

Figure 5 shows the trajectory of the WTG electric power under the proposed control strategy, where P_{We} , P_{Wm} , and P_{WMPPT} are the output electric power, the mechanical power of the turbine, and the power order of the MPPT control, respectively. The WTG operates at point A before the frequency regulation. When a power shortage occurs, the system frequency drops and the WTG electric power increases according to its control strategy and comes to point B. Since the WTG electric power is higher than the mechanical power, it will decelerate and come to point C. At point C, the WTG electric power is equal to the mechanical power. Then, the WTG electric power will continue to decrease and become lower than the mechanical power. After that, the rotor will accelerate and comes to point D. At point D, the WTG electric power is equal to the MPPT power order. Then, the WTG switches back to the MPPT mode and returns to point A with MPPT control.

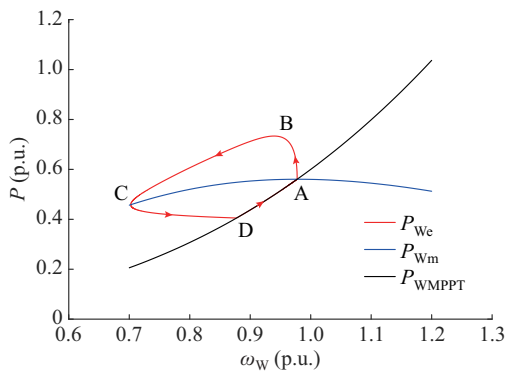


Fig. 5. Trajectory of WTG electric power under proposed control strategy.

From the process, we can know that the proposed control strategy has three advantages.

- 1) The WTG increases the electric power to support fre-

quency quickly after the frequency drop.

2) The WTG decreases the electric power automatically after supporting frequency to avoid its rotor speed being too low.

3) The WTG returns to the original operating point after the frequency regulation to ensure that the steady-state frequency is the same as that in the situation when WTG does not participate in the frequency regulation.

The proposed control strategy achieves a good balance between the frequency support and rotor speed recovery.

The steady-state frequency remains the same as that in the situation when WTG does not participate in the frequency regulation. The WTG supports the system frequency only temporarily, but its rotor kinetic energy is released at the most appropriate time. Therefore, a higher frequency nadir and better SFR are obtained.

IV. INFLUENCE OF CONTROL PARAMETERS ON SYSTEM FREQUENCY AND THEIR SENSITIVITY TO SYSTEM FREQUENCY

Section III provides a parameter setting method for the proposed strategy. According to [24], the coordination with SG is affected by K_{WD2} and T_{WD} , which are decided by the parameters of SG shown in Section III. K_{WD1} is decided by K_{WD2} and T_{WD} . The influence of K_{WD1} , K_{WD2} , and T_{WD} on the frequency is studied in this section.

To explore the influence of control parameters, a simulation is done in the four-generator two-area system. The structure of the system is shown in Fig. 6. G2 is a hydro generator, while G3 and G4 are thermal generators. The frequency dead zone values of the hydro generator and the thermal generators are ± 0.05 Hz and ± 0.033 Hz, respectively. The WTG model, SG model, and prime mover and governor model are taken from [25], [26], and [27], respectively. The WTG generation power accounts for 25% of the total system generation power. The disturbance in the system is a 10% power shortage. The wind speed is 8.5 m/s. Because there are multiple generators in the system, the system frequency as described below is actually system average frequency, which is the frequency of the center of inertia of the system.

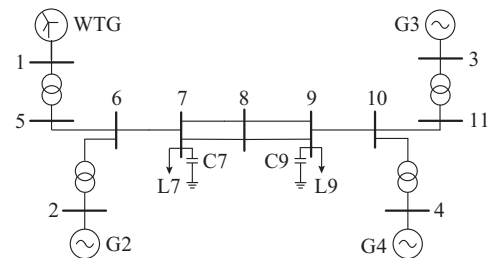


Fig. 6. Structure of simulation system.

When K_{WD1} , K_{WD2} , and T_{WD} are optimal, if K_{WD1} becomes bigger, K_{WD2} becomes smaller, or T_{WD} becomes bigger, the WTG rotor speed will drop to the minimum speed limit. Therefore, we only discuss the situations of smaller K_{WD1} , bigger K_{WD2} , or smaller T_{WD} .

It can be observed from Fig. 7 and Table I that when K_{WD1} decreases, the frequency nadir becomes lower, while the time for the frequency to reach the steady state is shortened.

It can be observed from Fig. 8 and Table II that when K_{WD2} increases, the frequency nadir becomes lower, while the time for the frequency to reach the steady state is shortened. It can be observed from Fig. 9 and Table III that when T_{WD} decreases, the frequency nadir becomes lower, while the time for the frequency to reach the steady state is shortened.

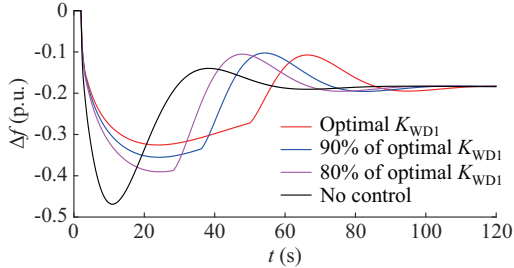


Fig. 7. Comparison of system frequency with different K_{WD1} .

TABLE I
COMPARISON OF FREQUENCY NADIR WITH DIFFERENT K_{WD1}

Parameter	min Δf (Hz)	Improvement of proposed control strategy relative to no control (%)
Optimal K_{WD1}	-0.3253	30.61
90% of optimal K_{WD1}	-0.3552	24.24
80% of optimal K_{WD1}	-0.3904	16.72
No control	-0.4688	0

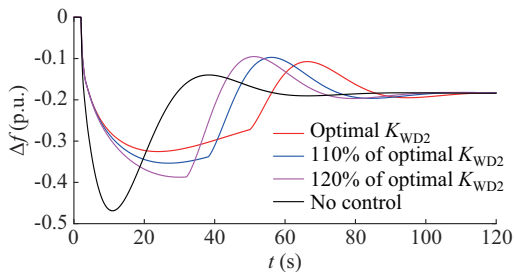


Fig. 8. Comparison of system frequency with different K_{WD2} .

TABLE II
COMPARISON OF FREQUENCY NADIR WITH DIFFERENT K_{WD2}

Parameter	min Δf (Hz)	Improvement of proposed control strategy relative to no control (%)
Optimal K_{WD2}	-0.3253	30.61
110% of optimal K_{WD2}	-0.3535	24.60
120% of optimal K_{WD2}	-0.3874	17.36
No control	-0.4688	0

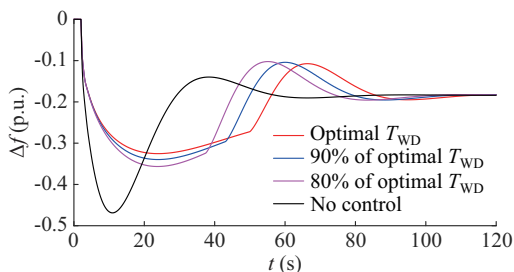


Fig. 9. Comparison of system frequency with different T_{WD} .

TABLE III
COMPARISON OF FREQUENCY NADIR WITH DIFFERENT T_{WD}

Parameter	min Δf (Hz)	Improvement of proposed control strategy relative to no control (%)
Optimal T_{WD}	-0.3253	30.61
90% of optimal T_{WD}	-0.3396	27.56
80% of optimal T_{WD}	-0.3565	23.96
No control	-0.4688	0

The sensitivity comparison of minimum frequency to different control parameters is shown in Table IV. The sensitivity refers to the percentage of change of the lowest frequency of the system when the control parameters change by 1%. From Table IV, it can be observed that the system frequency nadir is more sensitive to K_{WD1} and K_{WD2} than that to T_{WD} .

TABLE IV
SENSITIVITY COMPARISON OF MINIMUM SYSTEM FREQUENCY TO DIFFERENT CONTROL PARAMETERS

Parameter	Sensitivity
K_{WD1}	0.92
K_{WD2}	-0.87
T_{WD}	0.44

V. ADAPTABILITY OF PROPOSED CONTROL STRATEGY TO MULTIPLE SCENARIOS

To verify the effectiveness and adaptability of the proposed control strategy to multiple scenarios, simulations of various scenarios are done in this section. All of these scenarios are compared with a benchmark scenario in aspects of the disturbance types and severity, WTG control parameters, and the WTG operation condition. All simulations are done in the four-generator two-area system shown in Fig. 6. The synthetic inertia control, which is a variable coefficient integrated inertia control, is taken from [14]. The values of the droop control coefficient and virtual inertia control coefficient change with the WTG rotor speed.

A. Benchmark Scenario

In the benchmark scenario, the WTG generation power accounts for 25% of the total system generation power. The disturbance in the system is a 10% power shortage. The wind speed is 8.5 m/s. The comparison of the system frequency between the optimal control and synthetic inertia control is shown in Fig. 10.

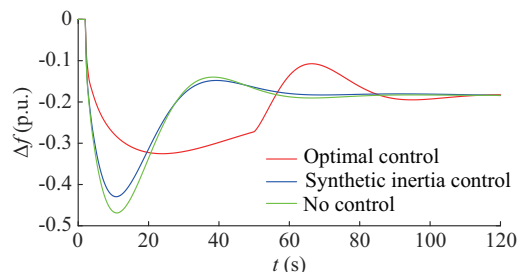


Fig. 10. Comparison of system frequency of benchmark scenario.

The comparison of the WTG rotor speed in the benchmark scenario is shown in Fig. 11, while the comparison of the WTG electric power in the benchmark scenario is shown in Fig. 12.

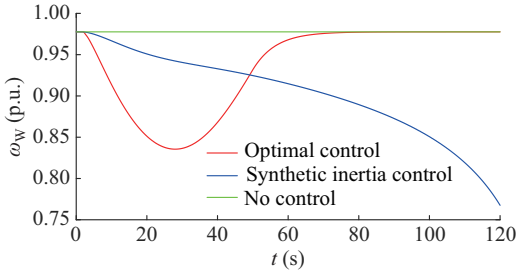


Fig. 11. Comparison of WTG rotor speed in benchmark scenario.

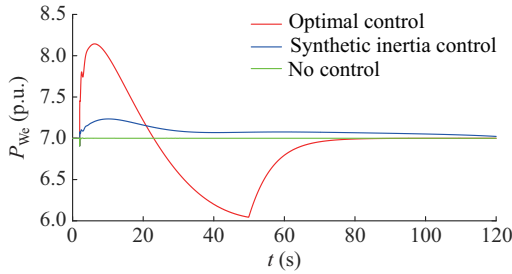


Fig. 12. Comparison of WTG electric power in benchmark scenario.

As shown in Fig. 11, if the synthetic inertia control is adopted, the WTG rotor speed will drop all the time. If the WTG rotor speed decelerates to the minimum speed limit and the WTG switches back to the MPPT mode, the electric power drop and secondary frequency drop in the system will be caused, which will deteriorate the frequency nadir. To avoid the deterioration of SFR caused by the secondary frequency drop, the electric power increment of the synthetic inertia control should not be too large to avoid too fast drop of WTG rotor speed.

It will restrain the frequency support effect of synthetic inertia control. However, if the proposed control strategy is adopted, the WTG rotor speed will return to the initial speed at the end of frequency regulation, which will not cause a negative power impact on the system and achieve a much better balance between the frequency support and WTG rotor speed. This is because the proposed control strategy considers the limited rotor kinetic energy at the beginning of the design to overcome the drawback of the auxiliary frequency control strategy of WTG using rotor kinetic energy. It realizes the reasonable allocation of the limited frequency regulation energy of WTG and its coordination with SG in the primary frequency regulation.

It can be observed from Fig. 11 and Fig. 12 that if the proposed control strategy is adopted for the WTG, the electric power will increase rapidly in the early stage of the frequency regulation to support the system frequency, and then the electric power will decrease to recover the rotor speed.

In the later period of frequency regulation, the frequency regulation power of the SG has been fully released. At this time, the main task of the WTG is to quickly reduce the

electric power to below the mechanical power to restore the rotor speed without causing the secondary frequency drop.

The proposed control strategy can make the frequency regulation of the WTG and SG achieve better coordination. In comparison, if the synthetic inertia control in [14] is adopted for the WTG, the electric power in the whole process of frequency regulation is higher than the mechanical power, so that the rotor speed decreases continuously and the mechanical power decreases. Although the coefficients of synthetic inertia control decrease as the rotor speed decreases, the electric power is still higher than the mechanical power. Therefore, it is difficult for the WTG to recover the initial speed after the frequency regulation, and it may even lead to a secondary frequency drop. The limited rotor kinetic energy of the WTG is not reasonably distributed in the frequency regulation process under the synthetic inertia control, but it is much better distributed under the optimal control.

B. Different Types of Disturbances

Two different types of disturbances, i.e., the 5% power shortage disturbance and the 5% power surplus disturbance, are tested in this subsection. The optimal control parameters of the WTG remain the same as the benchmark scenario of a 10% power shortage.

For the power shortage disturbance, it can be observed from Fig. 13 and Fig. 14 that the frequency nadir of the proposed control strategy is still better than the synthetic inertia control, while the rotor speed decelerates less than the benchmark scenario. Parameters of the more severe situation can be applied to the less severe situation. Therefore, the parameters can be set by considering the maximum power shortage in the system.

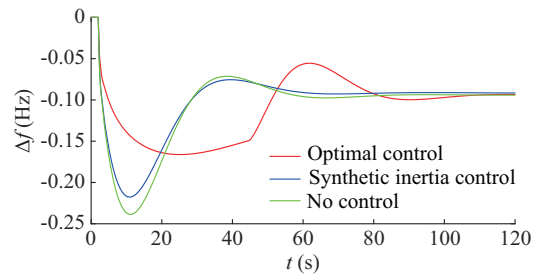


Fig. 13. Comparison of system frequency under 5% power shortage disturbance.

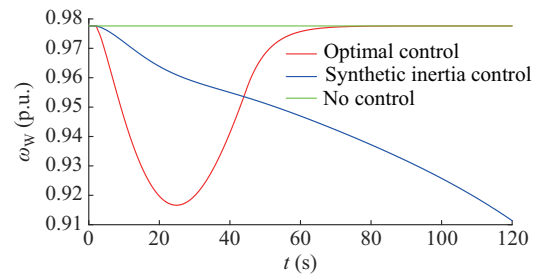


Fig. 14. Comparison of WTG rotor speed under 5% power shortage disturbance.

For the power surplus disturbance, it can be observed

from Fig. 15 that the maximum frequency of the proposed control strategy is lower than that of the synthetic inertia control. It can be observed from Fig. 16 that the rotor speed can return to the original value before the frequency regulation. Meanwhile, it can be observed from Fig. 17 that the comparison of WTG electric power of 5% power surplus disturbance. Thus, the proposed control strategy can also be applied to the situation of power surplus disturbance.

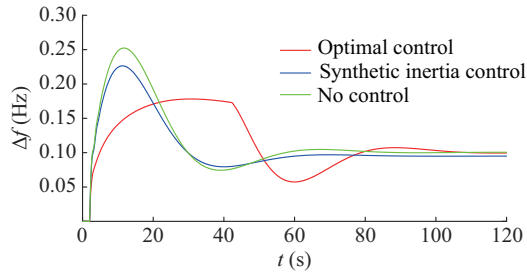


Fig. 15. Comparison of system frequency under 5% power surplus disturbance.

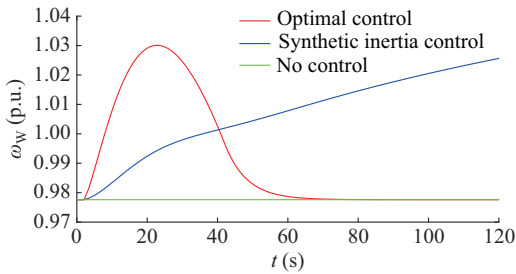


Fig. 16. Comparison of WTG rotor speed under 5% power surplus disturbance.

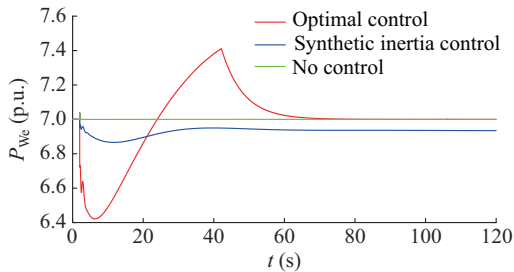


Fig. 17. Comparison of WTG electric power under 5% power surplus disturbance.

C. Decrease of Wind Speed

A lower wind speed (8 m/s) within the range when WTG adopts the MPPT control is verified in this subsection. When the wind speed decreases, the WTG rotor decelerates and its kinetic energy decreases. Therefore, K_{WD1} should be smaller when the wind speed decreases.

It can be observed from Fig. 18 that in the scenario of lower wind speed, the proposed control strategy still performs well. The frequency nadir is improved compared with the synthetic inertia control. Meanwhile, the rotor speed can return to the original value after the frequency regulation, as shown in Fig. 19. Thus, the proposed control strategy can be applied to the scenario of lower wind speed as well. The

WTG rotor speed does not decrease below the minimum speed limit when the wind speed decreases owing to the decrease of K_{WD1} .

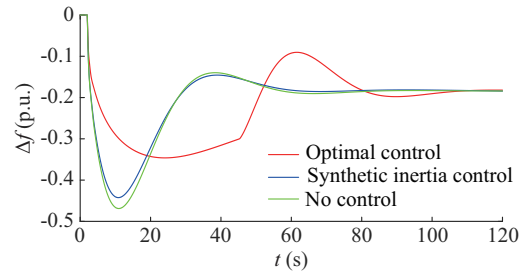


Fig. 18. Comparison of system frequency with lower wind speed.

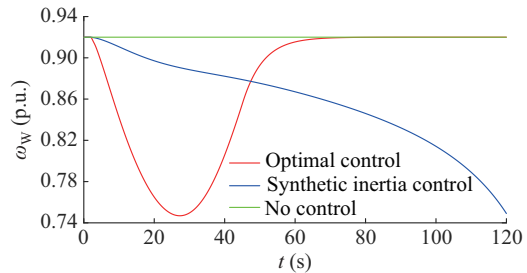


Fig. 19. Comparison of WTG rotor speed with lower wind speed.

D. Inaccurate System Model Parameters

Assume that the system model parameters have a random 10% error. Use the parameters of the benchmark scenario to obtain the WTG control parameters and derive the SFR.

It can be observed from Fig. 20 that even if system model parameters are inaccurate, the frequency nadir of the proposed control strategy is higher than that of the synthetic inertia control. Therefore, the proposed control strategy can adjust to the inaccuracy of system model parameters, which demonstrates that the proposed control strategy is robust to system parameters.

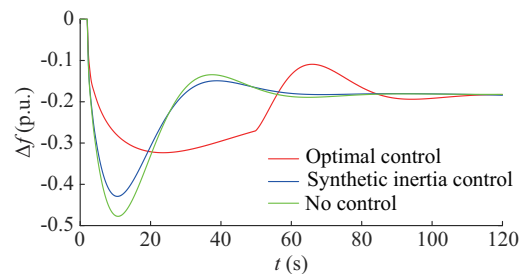


Fig. 20. Comparison of system frequency with inaccurate system model parameters.

E. Summary

Table V presents the comparison of frequency nadir (frequency peak value for power surplus) of the proposed control strategy and synthetic inertia control of WTG in various scenarios. It can be observed from Table V that in all scenarios, the improvement of the proposed control strategy relative to synthetic inertia control is significant.

TABLE V
COMPARISON OF FREQUENCY NADIR OF PROPOSED CONTROL STRATEGY AND SYNTHETIC INERTIA CONTROL OF WTG

Scenario	min Δf (max Δf for power surplus) (Hz)			Improvement of proposed control strategy relative to synthetic inertia control (%)
	No control	Synthetic inertia control	Proposed control strategy	
Benchmark scenario	-0.4688	-0.4295	-0.3253	22.23
5% power shortage	-0.2387	-0.2176	-0.1662	21.53
5% power surplus	0.2523	0.2264	0.1781	19.14
Lower wind speed (8 m/s)	-0.4688	-0.4424	-0.3462	20.52
Inaccurate system model parameters	-0.4776	-0.4292	-0.3234	22.16

VI. CONCLUSION

In this paper, the functional optimization model of the optimal auxiliary frequency control strategy of WTG is established and numerically solved. The form of the control strategy is proposed and studied. A practical optimal auxiliary frequency control strategy of WTG is proposed. The proposed control strategy makes full use of the advantages of WTG and SG, which has the following advantages.

1) The control strategy is concise and easy to implement. After the frequency transient support, the WTG returns to the MPPT mode. Therefore, it can be well integrated into the WTG power control link.

2) The secondary frequency drop is avoided as the WTG smoothly switches between the MPPT mode and frequency regulation mode. The WTG electric power can drop automatically after the frequency support.

3) The coordination of WTG and SG in the frequency regulation is enhanced by the proposed control strategy. The frequency regulation of WTG is fast but the available energy is limited while the frequency regulation ability of SG is enough but the response is slow. The proposed control strategy combines the advantages of WTG and SG and obtains better SFR.

4) The proposed control strategy adapts to different disturbances and different wind speeds. It is also robust to system parameters. Therefore, the proposed control strategy can adapt to different working conditions of the power system.

However, the coordination between different WTGs is also a very complex problem. Different WTGs have different working conditions with different frequency regulation abilities. Therefore, a control strategy to coordinate the auxiliary frequency control of different WTGs is required and will be our future work.

REFERENCES

- [1] Y. Yoo, S. Jung, and G. Jang, "Dynamic inertia response support by energy storage system with renewable energy integration substation," *Journal of Modern Power Systems and Clean Energy*, vol. 8, no. 2, pp. 260-266, Mar. 2020.
- [2] W. Yan, X. Wang, W. Gao *et al.*, "Electro-mechanical modeling of wind turbine and energy storage systems with enhanced inertial response," *Journal of Modern Power Systems and Clean Energy*, vol. 8, no. 5, pp. 820-830, Sept. 2020.
- [3] H. Xu, C. Yu, C. Liu *et al.*, "An improved virtual inertia algorithm of virtual synchronous generator," *Journal of Modern Power Systems and Clean Energy*, vol. 8, no. 2, pp. 377-386, Mar. 2020.
- [4] A. Zertek, G. Verbic, and M. Pantos, "A novel strategy for variable-speed wind turbines' participation in primary frequency control," *IEEE Transactions on Sustainable Energy*, vol. 3, no. 4, pp. 791-799, Oct. 2012.
- [5] K. V. Vidyandandan and N. Senroy, "Primary frequency regulation by deloaded wind turbines using variable droop," *IEEE Transactions on Power Systems*, vol. 28, no. 2, pp. 837-846, May 2013.
- [6] A. B. T. Attya and T. Hartkopf, "Control and quantification of kinetic energy released by wind farms during power system frequency drops," *IET Renewable Power Generation*, vol. 7, no. 3, pp. 210-224, May 2013.
- [7] G. Ramtharan, J. B. Ekanayake, and N. Jenkins, "Frequency support from doubly fed induction generator wind turbines," *IET Renewable Power Generation*, vol. 1, no. 1, pp. 3-9, Mar. 2007.
- [8] J. F. Conroy and R. Watson, "Frequency response capability of full converter wind turbine generators in comparison to conventional generation," *IEEE Transactions on Power Systems*, vol. 23, no. 2, pp. 649-656, May 2008.
- [9] D. Gautam, L. Goel, R. Ayyanar *et al.*, "Control strategy to mitigate the impact of reduced inertia due to doubly fed induction generators on large power systems," *IEEE Transactions on Power Systems*, vol. 26, no. 1, pp. 214-224, Feb. 2011.
- [10] S. Ghosh, S. Kamalasadana, N. Senroy *et al.*, "Doubly fed induction generator (DFIG)-based wind farm control framework for primary frequency and inertial response application," *IEEE Transactions on Power Systems*, vol. 31, no. 3, pp. 1861-1871, May 2016.
- [11] R. You, J. Y. Chai, X. Sun *et al.*, "Variable speed wind turbine based on electromagnetic coupler and its experimental measurement," in *Proceedings of 2014 IEEE PES General Meeting*, National Harbor, USA, Jul. 2014, pp. 1-5.
- [12] D. Sun, H. Liu, S. Gao *et al.*, "Comparison of different virtual inertia control methods for inverter-based generators," *Journal of Modern Power Systems and Clean Energy*, vol. 8, no. 4, pp. 768-777, Jul. 2020.
- [13] W. Li, M. Yin, Z. Chen *et al.*, "Inertia compensation scheme for wind turbine simulator based on deviation mitigation," *Journal of Modern Power Systems and Clean Energy*, vol. 5, no. 2, pp. 228-238, Mar. 2017.
- [14] J. Lee, E. Muljadi, P. Srensen *et al.*, "Releasable kinetic energy-based inertial control of a DFIG wind power plant," *IEEE Transactions on Sustainable Energy*, vol. 7, no. 1, pp. 279-288, Jan. 2016.
- [15] I. D. Margaritis, S. A. Papathanassiou, N. D. Hatzigiorgiou *et al.*, "Frequency control in autonomous power systems with high wind power penetration," *IEEE Transactions on Sustainable Energy*, vol. 3, no. 2, pp. 189-199, Apr. 2012.
- [16] M. Kayikci and J. V. Milanovic, "Dynamic contribution of DFIG-based wind plants to system frequency disturbances," *IEEE Transactions on Power Systems*, vol. 24, no. 2, pp. 859-867, May 2009.
- [17] G. C. Tarnowski, P. C. Kjar, P. E. Sorensen *et al.*, "Variable speed wind turbines capability for temporary over-production," in *Proceedings of 2009 IEEE PES General Meeting*, Calgary, Canada, Jul. 2009, pp. 1-7.
- [18] J. Morren, S. W. H. de Haan, W. L. Kling *et al.*, "Wind turbines emulating inertia and supporting primary frequency control," *IEEE Transactions on Power Systems*, vol. 21, no. 1, pp. 433-434, Feb. 2006.
- [19] W. Bao, Q. Wu, L. Ding *et al.*, "Synthetic inertial control of wind farm with BESS based on model predictive control," *IET Renewable Power Generation*, vol. 14, no. 13, pp. 2447-2455, Oct. 2020.
- [20] Y. Ye, Y. Qiao, and Z. Lu, "Revolution of frequency regulation in the converter-dominated power system," *Renewable and Sustainable Energy Reviews*, vol. 111, pp. 145-156, Sept. 2019.
- [21] F. Liu, Z. Liu, S. Mei *et al.*, "ESO-based inertia emulation and rotor speed recovery control for DFIGs," *IEEE Transactions on Energy Conversion*, vol. 32, no. 3, pp. 1209-1219, Sept. 2017.
- [22] Y. Yao, F. Liu, Z. Liu *et al.*, "Nonlinear droop control of VSWTs for

- sustained frequency regulation,” *Power System Technology*, vol. 42, no. 6, pp. 1845-1852, Jun. 2018.
- [23] H. Gao, P. Zi, L. Huang *et al.*, “Optimal frequency control of grid-connected power electronic devices with energy constraints,” *Automation of Electric Power Systems*, vol. 44, no. 17, pp. 9-18, Sept. 2020.
- [24] M. Sun, F. Xu, L. Chen *et al.*, “Optimal auxiliary frequency control strategy of wind turbine generator utilizing rotor kinetic energy,” *Proceedings of the CSEE*, vol. 41, no. 2, pp. 506-514, Jan. 2021.
- [25] M. Sun, Y. Min, L. Chen *et al.*, “A critical study on optimal auxiliary frequency control of wind turbine generator and coordination with synchronous generator,” *CSEE Journal of Power and Energy Systems*, vol. 7, no. 1, pp. 78-85, Jan. 2021.
- [26] L. Chen, Y. Min, Y. Chen *et al.*, “Evaluation of generator damping using oscillation energy dissipation and the connection with modal analysis,” *IEEE Transactions on Power Systems*, vol. 29, no. 3, pp. 1393-1402, May 2014.
- [27] X. Lu, L. Chen, Y. Chen *et al.*, “Ultra-low-frequency oscillation of power system primary frequency regulation,” *Automation of Electric Power Systems*, vol. 41, no. 16, pp. 64-70, Aug. 2017.

Ming Sun received the B.S. degree in electrical engineering from the Department of Electrical Engineering, Tsinghua University, Beijing, China, in 2016, where he is currently pursuing the Ph.D. degree in electrical engineering. His research interests include power system frequency security and auxiliary frequency control of renewable energy.

Yong Min received the B.S. and Ph.D. degrees in electrical engineering in the Department of Electrical Engineering, Tsinghua University, Beijing, China, in 1984 and 1990, respectively. He is currently a Professor in the Department of Electrical Engineering, Tsinghua University. He is a Fellow of the Institution of Engineering and Technology. His research interests include power system dynamic analysis and smart grid.

Xuejun Xiong received the B.S. and M.S. degrees in electrical engineering from Huazhong University of Science and Technology, Wuhan, China, in 2013 and 2016, respectively. She is now working at State Grid Shanghai Electric Power Research Institute, Shanghai, China. Her research interests include power grid security management, stability analysis and control, new energy resource integration.

Lei Chen received the B.Sc. and Ph.D. degrees in electrical engineering from Tsinghua University, Beijing, China, in 2003 and 2008, respectively. Since 2008, he has been with the Department of Electrical Engineering, Tsinghua University, where he is currently an Associate Professor. He was a recipient of the Excellent Young Scientists Fund of the National Natural Science Foundation of China in 2019. His research interests include dynamic analysis and control of power systems.

Le Zhao received the M.S. degree in electrical engineering from Shanghai University of Electric Power, Shanghai, China, in 2017. He is now working at State Grid Shanghai Electric Power Research Institute, Shanghai, China. His research interests include power grid security management, stability analysis and control, and new energy resource integration.

Yuyao Feng received the B.S. and M.S. degrees in electrical engineering from Shanghai Jiao Tong University, Shanghai, China, in 2005 and 2008, respectively. He is now working at State Grid Shanghai Electric Power Research Institute, Shanghai, China. His research interests include power grid security management, stability analysis and control, and new energy resource integration.

Bingran Wang is an undergraduate student majored in electrical engineering at Harbin Institute of Technology (Weihai), Weihai, China. He is currently participating in joint research with Tsinghua University, Beijing, China. His research interests include power system stability and control.